

A critical analysis of the ground and excited electronic states of transition metal nitrides using the relativistic effective Hamiltonian method

Rajat K. Chaudhuri

Indian Institute of Astrophysics, Bangalore-560034, India

Karl F. Freed

The James Franck Institute and the Department of Chemistry, The University of Chicago, Chicago, Illinois 60637

(Received 27 January 2003; accepted 20 June 2003)

Multireference many-body perturbative schemes (IVO-CASCI and H_v^{3rd}), which are applicable to the direct calculation of excitation energies, ionization potentials, and spectroscopic properties, are presented and applied to compute the transition energies, ionization potentials, and spectroscopic constants of TiN and VN. Highly satisfactory results are obtained for the excitation energies, triple bond dissociation energy, dipole moments, oscillator strengths, and vibrational frequencies. The ground and excited properties of interest are also computed using Hartree-Fock and two-component Dirac-Hartree-Fock molecular orbitals to assess the importance of relativistic effects. We also report the ionization potentials of TiN^+ and VN^+ which are by-products of this method with “no extra” computational cost and which have not been studied previously. © 2003 American Institute of Physics. [DOI: 10.1063/1.1600432]

I. INTRODUCTION

The study of physical and chemical processes in atomic and molecular systems containing heavy elements is of great importance both experimentally and theoretically. Aside from their obvious relevance to understanding the chemistry of compounds containing heavy atoms, these studies can provide a quantitative estimate of relativistic contributions, kinematic effects, and a probe for physics that departs from the predictions of the *standard model*. The twin facts that heavy atom compounds contain many electrons and that the behavior of these electrons must be treated relativistically introduce severe impediments to accurate theoretical treatments (i.e., to the inclusion of sufficient electron correlation) of polyatomic systems containing heavy atoms. Rigorous relativistic electronic structure methods begin by foregoing the Schrödinger equation in favor of the Dirac equation, resulting in the replacement of nonrelativistic orbitals with four component relativistic spinors. The concomitant size of the matrices to be manipulated and the number of two-electron integrals to be evaluated in the four component Dirac equation have forced the introduction of various approximate method to describe the electronic structure of polyatomics containing heavy atoms by either restricting the number of electrons to be treated explicitly or by converting the relativistic problem into a combination of a nonrelativistic many electron problem, a perturbative treatment of the relativistic corrections, and/or both.

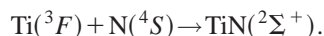
The most widely used approximate relativistic scheme for describing heavy atom systems is the *effective core potential* (ECP) method, where the core electrons are represented by suitable functions and where only the valence electrons are treated explicitly. Since the core changes insignificantly with the chemical environment, the ECP scheme provides quite good results at reduced computational

cost compared to all-electron calculations. The two widely used classes of ECP schemes are the pseudopotential and model potential methods. The pseudopotential method is derived from the Phillips-Kleinman (PK) equations,¹ where the valence orbitals are replaced by a set of nodeless pseudo-orbitals. The valence orbitals of the pseudopotential scheme are designed to behave correctly only in the outer region. Because the *ab initio model potential* (AIMP) method² describes the correct behavior for the inner nodal structure of the orbitals and because the relativistic operators act in the near vicinity of the nucleus, the AIMP orbitals emerge as more suitable than the pseudopotential orbitals.

Recently, Motegi *et al.* have proposed a somewhat less approximate relativistic scheme (RESC)³ for generating relativistic spinors. The RESC method proceeds by eliminating the small component portion of the relativistic Hamiltonian from the four-component Dirac equation through a suitable transformation. The RESC scheme is variationally stable and avoids the Coulomb singularity. Moreover, the formalism can be incorporated directly into any nonrelativistic electronic structure method since the implementation of the spin-free RESC Hamiltonian in *ab initio* programs merely requires only minor modification of the one-electron integrals. We compute and compare to prior nonrelativistic calculations the transition energies, oscillator strengths, and relevant spectroscopic constants of TiN and VN as obtained from separate calculations with nonrelativistic and with RESC molecular orbitals to estimate the magnitudes of the relativistic corrections. The Ti and V atoms are chosen as simple test cases because these atoms are not too heavy and, instead, lie on the border line where relativistic effects just begin to contribute. In addition, the TiN and VN systems provide an application involving the nontrivial problem of describing the correct dissociation for a triple bond.

We employ the highly correlated effective valence shell Hamiltonian (H^v) method through third order along with our recently developed, more approximate IVO-CASCI approach to generate the ground and excited potential energy curves and to compare the transition energies and spectroscopic constants with experiment and with other nonrelativistic correlated treatments. Besides providing the first correlated molecular application of the RESC Hamiltonian, we present computations for oscillator strengths and for several excited and ion states not previously treated. The study of the electronic structure of transition metal atoms and their compounds is nontrivial because the ground and the excited states of these systems are highly open-shell in nature and because a large number of electrons must be correlated to describe the ground and excited electronic states accurately. Moreover, the excited state spectrum of these systems generally contains states of qualitatively different spatial character, such as Rydberg and valence states and ionic and covalent states, thereby, introducing additional complexity in computations for the electronic states of these systems. As mentioned above, transition metal elements in the first series are border line elements where relativistic effect may be small but non-negligible. They also contain few enough electrons to enable treatment with correlated *ab initio* all-electron methods. Thus, these systems provide a useful first test for the use of relativistic methods to improve the description of their electronic states and their compounds. The treatment of compounds containing second row transition metal elements and lanthanides is more complicated because of the presence of more electrons and larger relativistic effects.

The ground state of TiN has ${}^2\Sigma^+$ symmetry and consists of a triple bond and one unpaired electron occupying a σ orbital located primarily on Ti. Combining the electronic states of the atoms and a population analysis leads to the suggestion that the adiabatic formation of the TiN ground state proceeds via



As the Ti atom approaches the nitrogen atom, the atomic F state of Ti splits into states of Σ^- , Π , Δ , and Φ symmetry, and the Σ^- state component of the polarized metal atom combines with the ground state of N to form the TiN (${}^2\Sigma^+$) ground state. A triple bond is formed from three singlet coupled electron pairs, leaving one of the high-spin N electrons unpaired. Thus, the three bonding orbitals and the singly occupied nonbonding orbital of TiN are formed from the union of five electrons from the high-spin nitrogen atom ground state and two electrons from the Ti atom with its remaining singlet coupled $4s$ electron pair. This transformation between the asymptotic atomic states and the molecular ground state is quite nontrivial because the interaction between the Ti and N atoms must excite a metal $4s$ electron to the metal $4p_\sigma$ orbital and transfer electron density to the nitrogen $2p_\sigma$ orbital in order to reduce the Pauli repulsion between the Ti $4s^2$ and nitrogen $2p_\sigma$ orbitals. The formation of the triple bond in the VN (${}^3\Delta$) ground state from the

separated V(4F) and N(4S) atoms is similar to that of TiN except that the additional electron goes into a V($3d_\sigma$) orbital.

Section II briefly reviews the RESC method, some essential features of the H^v method, and the procedure for generating the improved virtual orbitals (IVOs). Computational details and results follow in the subsequent section. To our knowledge, no prior computations are available for oscillator strengths and for the electronic structures of TiN^+ and VN^+ . Since correlated calculations for the low lying ion states emerge as simple by-products of the H^v computations for the neutral molecule and since TiN^+ and VN^+ are likely candidate to exist in stellar atmospheres, we include a description of the electronic structure of low lying TiN^+ and VN^+ electronic states.

II. THEORY

A. The RESC method

Because the details of the RESC scheme are available elsewhere,³ we only outline the essential content of the method here. The RESC Hamiltonian can be decomposed into spin-free (sf) and spin-dependent (sd) components as

$$H_{\text{RESC}} = H_{\text{RESC}}^{\text{sf}} + H_{\text{RESC}}^{\text{sd}}, \quad (2.1)$$

where

$$H_{\text{RESC}}^{\text{sf}} = \sum_j T_j + O_j Q_j \mathbf{p}_j \cdot V(j) \mathbf{p}_j Q_j O_j^{-1} + 2mc O_j Q_j^{1/2} V(j) Q_j^{1/2} O_j^{-1}, \quad (2.2)$$

and

$$H_{\text{RESC}}^{\text{sd}} = i \sum_j O_j Q_j \sigma \cdot (\mathbf{p}_j V(j) \times \mathbf{p}_j Q_j O_j^{-1}), \quad (2.3)$$

in which σ represents the 2×2 Pauli matrix and p_j is the momentum operator. The operators O_j , Q_j , and T_j are given by

$$O_j = \frac{1}{E_j + mc^2} \left[1 + \frac{p_j^2 c^2}{(E_j + mc^2)^2} \right]^{1/2}, \quad (2.4)$$

$$Q_j = \frac{1}{E_j + mc^2}, \quad (2.5)$$

$$T_j = \sqrt{p_j^2 c^2 + m^2 c^4} - mc^2, \quad (2.6)$$

and

$$E_j = \sqrt{p_j^2 c^2 + m^2 c^4}. \quad (2.7)$$

In the RESC scheme, the Hamiltonian elements are evaluated in the space spanned by the eigenfunction of p^2 (square of the momentum) as suggested by Buenker *et al.*⁴ The atomic RESC-AIMP Hamiltonian for n valence electron is written as

$$H^{\text{RESC-AIMP}} = \sum_{i=1}^n h(i) + \sum_{i < j} \frac{1}{r_{ij}}, \quad (2.8)$$

where

$$h(i) = T_i + O_j Q_j \mathbf{p}_j \cdot V(j) \mathbf{p}_j Q_j O_j^{-1} + 2m_c O_j Q_j^{1/2} V(j) Q_j^{1/2} O_j^{-1} + U(i) + P(i). \quad (2.9)$$

Here, the first and second terms of Eq. (2.9) are taken from the $H_{\text{RESC}}^{\text{sf}}$ operator. The composite operator $U(i)$ is defined as

$$U(i) = V_{\text{Coul}}(i) + V_{\text{exch}}(i) + \frac{Z_{\text{core}}}{r_i}, \quad (2.10)$$

where $V_{\text{Coul}}(i)$ and $V_{\text{exch}}(i)$ represent the Coulomb and exchange interactions between the valence and Z_{core} core electrons. In this formalism, the nodal structures of the valence orbitals are realized through the projection operator $P(i)$, which is obtained from the core–valence orthogonality condition and is expressed as

$$P(i) = - \sum_c^{\text{core}} 2\epsilon_c |\phi_c\rangle \langle \phi_c|, \quad (2.11)$$

where ϕ_c and ϵ_c denote the core orbitals and core orbital energies, respectively. The derivations and computational techniques are provided in more detail by Nakajima *et al.*⁵

B. The H^v method

As in conventional many-body perturbation theory, the H^v method⁶ begins with the decomposition of the exact Hamiltonian H into the zeroth order Hamiltonian H_0 and the perturbation V ,

$$H = H_0 + V, \quad (2.12)$$

where H_0 is constructed as the sum of one-electron Fock operators described below. The full many-electron Hilbert space is then partitioned into an active (also called valence) space with projector P and its orthogonal complement with projector $Q = 1 - P$. The active space spans the space of all distinct configuration state functions involving a filled core and the remaining electrons distributed among the valence orbitals in all possible manners to ensure what is termed “completeness” of the active space. Hence, the orthogonal complement Q space contains all N -electron basis functions with at least one vacancy in a core orbital and/or at least one electron in an excited orbital. Thus, we classify the orbitals as either “core,” “valence,” or “excited,” where the doubly filled orbitals in P space are denoted as core, the partially filled orbitals of P space are valence, and the orbitals that are unoccupied in all active P -space functions are the excited orbitals. With the aid of the projectors P and Q , the H^v method transforms the full Schrödinger equation,^{7,8}

$$H\Psi_i = E_i\Psi_i, \quad (2.13)$$

into the P -space “effective valence shell” Schrödinger equation,

$$H^v\Psi_i^v = E_i\Psi_i^v, \quad (2.14)$$

where the effective operator H^v through third order is given by

$$H^v = PHP + \frac{1}{2}[V_{\text{eff}}^{(2)} + V_{\text{eff}}^{(3)} + \text{h.c.}], \quad (2.15)$$

in which h.c. designates the Hermitian conjugate of the preceding terms in square brackets and E_0^P is the zeroth order energy (see below) of the P -space state. Here, the operators $V_{\text{eff}}^{(2)}$ and $V_{\text{eff}}^{(3)}$ are defined as

$$V_{\text{eff}}^{(2)} = PVQ(E_0^P - QH_0Q)^{-1}VP, \quad (2.16)$$

$$V_{\text{eff}}^{(3)} = PVQ[(E_0^P - QH_0Q)^{-1}VQ(E_0^P - QH_0Q)^{-1} - (E_0^P - QH_0Q)^{-2}P]VP. \quad (2.17)$$

Apart from the reference (P) space, the only variability in all MR–MBPT methods lies in the choice of orbitals, orbital energies, and the definition of the zeroth order Hamiltonian H_0 since the perturbation approximation is completely determined by these choices. Generally, the zeroth order Hamiltonian is prescribed as a sum of one-electron operators,

$$H_0(i) = \sum_c |\phi_c\rangle \epsilon_c \langle \phi_c| + \sum_v |\phi_v\rangle \times \epsilon_v \langle \phi_v| + \sum_e |\phi_e\rangle \epsilon_e \langle \phi_e|, \quad (2.18)$$

in terms of the core (c), valence (v), and excited (e) orbitals and their corresponding orbital energies. At this point, we emphasize that unlike traditional MR–MBPT, the H^v method and its first order approximation based on the PHP term, called the IVO–CASCI method, use *multiple* Fock operators to define the valence orbitals.^{9–11} In this scheme, all the valence orbitals and orbital energies are obtained from $V^{(N-1)}$ potentials and, therefore, are on an equal footing as opposed to the unbalanced use of a mixture of HF occupied and virtual orbitals for the valence space. Moreover, in this method the zeroth order Hamiltonian H_0 is defined as

$$H_0(i) = \sum_c |\phi_c\rangle \epsilon_c \langle \phi_c| + \sum_v |\phi_v\rangle \times \bar{\epsilon}_v \langle \phi_v| + \sum_e |\phi_e\rangle \epsilon_e \langle \phi_e|, \quad (2.19)$$

to improve the perturbative convergence.^{12–16} The average valence orbital energy $\bar{\epsilon}_v$ is obtained from the original set of valence orbital energies by the democratic averaging,

$$\bar{\epsilon}_v = \frac{\sum_i^{N_v} \epsilon_i}{N_v}, \quad (2.20)$$

with N_v the number of valence orbitals spanning the complete active P space (CAS). Prior applications of the IVO–CASCI method demonstrate that it produces comparable accuracy to CASSCF treatments with the same choice of valence space (of course, using different valence orbitals) but with considerably reduced computer time since no iterations are necessary beyond an initial ordinary SCF calculation.^{17,18}

Since the IVOs play a key role in our scheme (mentioned above), we briefly outline their generation. More detailed discussion is presented elsewhere.^{17,18} In the IVO–CASCI procedure, the HF MOs (both occupied and unoccupied) are first determined by diagonalizing the reference state Fock matrix ${}^1F_{lm}$,

TABLE I. IVO-CASCI and H_{3rd}^v vertical excitation energies (in eV) and the ground and excited states dipole moments (μ) and oscillator strengths (f) of TiN with the $[9\sigma 10\sigma 11\sigma 1\delta 4\pi]^1$ CAS. In this and all subsequent tables, the heading HF indicates the use of nonrelativistic orbitals. (The top entry for each state is obtained from the TZV basis, and the bottom is from Watcher's basis.)

| Properties | State | IVO-CASCI | | H_{3rd}^v | | Experiment |
|---------------------|---------------|-----------|-------|-------------|-------|--------------------|
| | | HF | RESC | HF | RESC | |
| Energy | $X^2\Sigma^+$ | 0.0 | 0.0 | 0.0 | 0.0 | 0.0 |
| | $B^2\Pi$ | 1.975 | 2.039 | 2.013 | 2.014 | 2.013 ^a |
| μ (Debye) | $X^2\Sigma^+$ | 2.046 | 2.107 | 1.962 | 1.986 | 3.56 ^b |
| | | 3.026 | 3.090 | 3.534 | 3.544 | |
| | $B^2\Pi$ | 2.898 | 2.972 | 3.521 | 3.479 | 4.6 ^b |
| | | 3.760 | 3.756 | 3.760 | 3.756 | |
| $f(X\rightarrow B)$ | | 3.584 | 3.590 | 3.590 | 3.584 | |
| | | 0.250 | 0.257 | 0.251 | 0.255 | |
| | | 0.268 | 0.263 | 0.250 | 0.248 | |

^aReference 24.

^bReference 25.

$${}^1F_{lm} = \langle \phi_l | h + \sum_{k=1}^{\text{occ}} (2J_k - K_k) | \phi_m \rangle = \delta_{lm} \epsilon_l, \quad (2.21)$$

where l and m designate any (occupied or unoccupied) HF MOs and ϵ_l is the HF orbital energy. The IVOs are determined variationally by minimizing the low lying singly excited $\Psi_{\alpha\rightarrow\mu}$ (α is the highest occupied MO) state energies with respect to a new set of MOs $\{\chi\}$. However, to ensure the orthogonality and applicability of Brillouin's theorem, the $\{\chi\}$ are expressed in terms of $\{\phi\}$ as

$$\chi_\alpha = \sum_{i=1}^{\text{occ}} a_{\alpha i} \phi_i, \quad \chi_\mu = \sum_{u=1}^{\text{unocc}} c_{\mu u} \phi_u. \quad (2.22)$$

It can be shown that setting $\{\chi_\alpha\} = \{\phi_\alpha\}$ (i.e., $a_{\alpha i} = \delta_{\alpha i}$) to be the occupied orbitals of the reference SCF configuration.

Then, the coefficients $c_{\mu u}$ in Eq. (2.22) can be determined directly from the matrix eigenvalue equation $F'C = CF$, where

$$F'_{vw} = {}^1F_{vw} + A_{vw}^\alpha, \quad (2.23)$$

$$A_{vw}^\alpha = \langle \chi_v | -J_\alpha + K_\alpha \pm K_\alpha | \chi_w \rangle, \quad (2.24)$$

and the minus(plus) sign applies for $\Psi_{\alpha\rightarrow\mu}$ a triplet(singlet) state.

III. RESULTS AND DISCUSSIONS

A. TiN

The TiN molecule has $C_{\infty v}$ symmetry with $R_{\text{TiN}} = 2.99 \text{ \AA}$ and with the z axis is defined as lying along TiN

TABLE II. Comparison of H_{3rd}^v vertical excitation energies (in eV) of TiN obtained from $[8\sigma 3\pi 9\sigma 1\delta 4\pi]^7$ CAS calculations. (The top entry for each state is obtained from the TZV basis, and the bottom is from Watcher's basis. Entries in parentheses are oscillator strengths for transitions from the ground state.)

| State | H_{3rd}^v | | | | | Experiment |
|---------------|---------------|--------------|------------------|-----------------|-----------------|--------------------|
| | HF | RESC | JFH ^a | CB ^b | SM ^c | |
| $X^2\Sigma^+$ | 0.000 | 0.000 | 0.000 | 0.000 | 0.00 | |
| | 0.000 | 0.000 | | | | |
| $A^2\Delta$ | 1.234 | 1.345 | 0.946 | 0.793 | 1.04 | 0.934 ^d |
| | 0.952 | 1.066 | | | | |
| $B^2\Pi$ | 1.998(0.027) | 2.082(0.030) | 2.010 | 2.010 | 1.95 | 2.013 ^e |
| | 2.051(0.038) | 2.149(0.042) | | | | |
| ${}^4\Delta$ | 2.742 | 2.736 | 1.850 | | | |
| | 2.693 | 2.687 | | | | |
| $B^2\Sigma^+$ | 2.832 | 2.746 | | | | 2.923 ^f |
| | 2.713 | 2.740 | | | | |
| $1^4\Pi$ | 2.585 | 2.629 | | | | |
| | 2.390 | 2.369 | | | | |
| $2^2\Pi$ | 2.884(0.0036) | 2.840(0.011) | | | | |
| | 2.665(0.0001) | 2.605(0.001) | | | | |
| $3^2\Pi$ | 3.054(0.031) | 3.052(0.028) | | | | |
| | 2.850(0.017) | 2.743(0.018) | | | | |
| $2^2\Sigma^+$ | 3.098 | 3.097 | | | | |
| | 3.232 | 3.123 | | | | |

^aReference 26.

^bReference 27.

^cReference 28.

^dReference 29.

^eReference 24.

^fReference 30.

TABLE III. Experimental and computed ground and excited state dipole moment (in Debye) of TiN.

| State | IVO-CASCI | | H_v^{3rd} | | JFH ^a | CB ^b | SM ^c | Experiment ^d |
|---------------|-----------|------|-------------|------|------------------|-----------------|-----------------|-------------------------|
| | HF | RESC | HF | RESC | | | | |
| $X^2\Sigma^+$ | 3.47 | 3.55 | 3.64 | 3.45 | 3.25 | 3.05 | 3.65 | 3.56 |
| $A^2\Delta$ | 4.49 | 4.44 | 4.95 | 4.81 | 7.84 | 7.86 | 6.83 | |
| $B^2\Pi$ | 4.04 | 4.07 | 4.58 | 4.56 | 4.43 | 4.48 | 4.30 | 4.63 |

^aReference 26.^bReference 27.^cReference 28.^dReference 25.

bond. Two sets of basis functions are employed to compute the excitation energies, ionization potentials and related molecular properties of TiN. The MOs that are used to compute the transition energies and molecular properties are obtained by solving the Hartree–Fock and two-component Dirac–Hartree–Fock (DHF) equations to estimate the relativistic contribution to the transition energies and related molecular properties, such as the equilibrium bond lengths (R_e), dissociation energies (D_e), etc. The first atomic basis is chosen as $(14s, 11p, 6d)/[10s, 8p, 3d]$ and $(10s, 6p)/[5s, 3p]$ contractions centered on the Ti and N atoms, respectively. This contraction scheme yields 66 contracted Gaussian-type orbitals (CGTOs) with the total HF and DHF energies $-902.718\,765\,4778$ a.u. and $-907.034\,141\,580$ a.u., respectively. For the larger Watcher’s basis, we employ $(14s, 11p, 6d, 3f)/[8s, 6s, 4d, 1f]$ contractions¹⁹ for Ti and an aug-cc-pVTZ basis²⁰ for the N atom. The computed HF and two-component HF energies with this basis (comprised of 115 CG–TOs) are $-902.731\,043\,4962$ a.u. and $-907.067\,296\,1501$ a.u., respectively. The ground state configuration of TiN ($X^2\Sigma$) is $[\text{core}]^{22} 8\sigma^2 3\pi^4 9\sigma$. Since ground state of TiN is open-shell with one-electron well separated from the inner core, we choose the closed-shell positive ion ground state configuration $[\text{core}]^{22} 8\sigma^2 3\pi^4$ as the vacuum (reference) state for convenience. In accord with numerous H^v calculations, tests for TiN demonstrate that the third order description is almost identical to that following from the use of the neutral ground state approximation as the reference state.

While the first excited state ($^2\Pi$) of TiN arises from a $9\sigma \rightarrow 4\pi^*$ transition (HOMO \rightarrow LUMO), the $^2\Sigma$ excited state arises from a $8\sigma \rightarrow 9\sigma$ excitation. Since the 8σ and 3π orbitals

are quasidegenerate, we include both 8σ and 3π orbitals in the reference space along with the 9σ , 1δ , and 4π molecular orbitals. Thus, the H^v reference space consists of seven electrons and seven valence orbitals ($8\sigma, 9\sigma, 1\delta, 3\pi$, and 4π). Clearly, this choice stems from the fact that the treatment of potential curves for the dissociation of a triply bonded species naturally calls for the inclusion of the three bonding and antibonding orbitals in the reference space. A second set of calculations is also performed where 8σ and 3π are included in the core for a quick estimation of the $^2\Pi$ state vertical excitation energy.

Table I reports the $9\sigma \rightarrow 4\pi^*$ vertical transition energy and the $X^2\Sigma^+$ and $B^2\Pi$ states dipole moment and oscillator strengths for $X \rightarrow B$ transition of TiN obtained from the IVO-CASCI and third order H_v methods using HF and RESC molecular orbitals. (In Tables I–VI, the column headed by HF is obtained using nonrelativistic orbitals.) The IVO-CASCI and H_v^{3rd} calculations for Table I have been performed with a seven orbital, one valence electron (9σ) reference space as a prelude to identify in a computationally inexpensive strategy the most appropriate sets of unoccupied valence orbitals for subsequent treatment of nondynamical correlation. While the single valence electron reference space IVO-CASCI and H_v^{3rd} calculations of Table I provide a highly accurate estimate of the $X^2\Sigma^+ \rightarrow B^2\Pi$ transition energy and the ground state dipole moment of TiN, they poorly describe the high-lying $^2\Sigma$ (also $^2\Delta$) excited states and energies because unlike the $B^2\Pi$ state, the $^2\Sigma$ state is not solely of $9\sigma \rightarrow 10\sigma$ parentage.

Table II compares the IVO-CASCI and H_v^{3rd} vertical excitation energies for TiN with experiment and with other

TABLE IV. Spectroscopic constants for the $X^2\Sigma^+$ ground and $^2\Delta$ first excited states of TiN.

| State | Spectroscopic constants | IVO-CASCI | JFH ^a | CB ^b | SM ^c | Experiment |
|---------------|-------------------------|-----------|------------------|-----------------|-----------------|--------------------|
| $X^2\Sigma^+$ | R_e (in a.u.) | 3.0746 | 3.048 | 3.080 | 2.963 | 2.990 ^d |
| | D_e (in eV) | 4.24 | 4.19 | 3.76 | | 4.9 ^e |
| | ω_e | 1045 | 1024 | 1010 | 1139 | 1039 ^f |
| $A^2\Delta$ | R_e (in a.u.) | 3.30 | 3.13 | 3.19 | 3.03 | |
| | D_e (in eV) | 3.24 | 4.05 | | | |
| | ω_e | 820 | 931 | 1020 | 990 | |

^aReference 26.^bReference 27.^cReference 28.^dReference 24.^eReference 31.^fReference 32.

TABLE V. H_{3rd}^v vertical excitation energies (in eV) of VN.

| State | Dominant configuration | H_{3rd}^v | | JFH ^a | Experiment |
|-------------|------------------------|-------------|-------|------------------|------------|
| | | HF | RESC | | |
| $X^3\Delta$ | $1\delta 9\sigma$ | 0.0 | 0.0 | | |
| $1^1\Sigma$ | $1\delta^2$ | 0.741 | 0.839 | 0.657 | |
| $1^1\Delta$ | $1\delta 9\sigma$ | 0.868 | 0.877 | | |
| $1^3\Pi$ | $1\delta 4\pi$ | 0.897 | 0.923 | | |
| $1^1\Pi$ | $3\pi 9\sigma$ | 1.814 | 1.772 | 1.582 | 1.774 |
| $1^3\Sigma$ | $9\sigma 10\sigma$ | 1.645 | 1.581 | | |
| $2^1\Sigma$ | $9\sigma 10\sigma$ | 1.831 | 1.839 | | |
| $2^1\Pi$ | $1\delta 4\pi$ | 1.961 | 1.991 | 2.11 | 2.259 |

^aReference 26.

theoretical calculations. Here, the IVO-CASCI and H_v^{3rd} transition energies and related properties are computed using the much larger CAS for describing properly and simultaneously the ground and excited state of interest through the appropriate incorporation of core-core, core-valence, and valence-valence dynamical electron correlation. The IVO-CASCI/ H_v reference space is constructed by allocating seven valence electrons (8σ , 9σ , and 3π occupied in the ground state) into seven valence orbitals (8σ , 9σ , 1δ , 3π , and 4π). The present calculation shows that the inclusion of the 8σ and 3π doubly occupied orbitals in the reference space more greatly impacts the IVO-CASCI than the H_v^{3rd} transition energies. For example, the inclusion of the 8σ and 3π doubly occupied orbitals in the reference space shifts the IVO-CASCI and third order H_v $X^2\Sigma \rightarrow B^2\Pi$ transition energy by 0.538 eV and 0.015 eV for nonrelativistic orbitals (0.436 eV and 0.068 eV for relativistic orbitals), respectively. Because the H_v^{3rd} method includes correlation contributions from all singly and doubly excited configurations with respect to any configuration in P space, the five-orbital valence space H_v^{3rd} treatment includes dynamical correlation contributions from the 8σ and 3π orbitals. Thus, the difference between the IVO-CASCI and H_v^{3rd} transition energies further suggests that dynamical electron correlation due to the 8σ and 3π orbitals is more important than is their contribution to nondynamical electron correlation. New calculations are provided for excited Π and Σ states that emerge from the H^v calculations simultaneously with the lower $^2\Sigma$ and $^2\Pi$ states and that have not been considered before. The present investigation also demonstrates that the inclusion of 8σ and 1π occupied orbitals in the reference space dramatically alters the oscillator strengths, a feature which is not unusual. Since neither experimental nor theoretical oscillator strengths are available for this system, the accuracy of our

computed oscillator strengths (displayed in Tables I and II) cannot be assessed apart from prior experience where good oscillator strengths are obtained.^{17,18,21-23}

Table III compares the IVO-CASCI and H_v^{3rd} dipole moments (μ) for the ground and excited states of TiN with experiment and with other theoretical estimates. The IVO-CASCI and H_{3rd}^v values reported in Table III are obtained using the $[8\sigma 3\pi 9\sigma 10\sigma 1\delta 4\pi]^7$ CAS calculations with Watcher's basis set. The present calculation exhibits the X and B state dipole moments obtained from the nonrelativistic and relativistic orbitals in favorable agreement with experiment and other correlated calculations. (Differences, however, are present for the $^2\Delta$ state dipole moment which is not available from experiment.) The above trends strongly suggests that the relativistic effects in TiN are negligible (as anticipated) and, hence, this system can be studied nonrelativistically. Though the single reference IVO-CASCI treatment provides a fairly accurate estimate of the $X^2\Sigma \rightarrow B^2\Pi$ transition energy, it poorly describes the corresponding dipole moments. The IVO-CASCI dipole moments are off by 0.53 Debye (0.47 Debye for relativistic orbitals) and by 0.87 Debye (0.874 Debye for relativistic orbitals) for the $X^2\Sigma$ and $B^2\Pi$ states, respectively. While the inclusion of dynamical electron correlation significantly reduces the estimated error for the $X^2\Sigma$ (0.026 Debye for HF MOs and 0.016 Debye for RESC MOs), the computed dipole moment for the $^2\Pi$ state remains the same. Inclusion of the 8σ and 1π occupied orbitals in the reference space significantly improves the accuracy of the $B^2\Pi$ excited state for both the IVO-CASCI and H_v^{3rd} calculations. The present work demonstrates that electron correlation (dynamical as well as non-dynamical) plays a key role in computing the excited state dipole moments.

Figure 1 depicts the computed IVO-CASCI potential

TABLE VI. H_{3rd}^v vertical ionization energies (in eV) of TiN and VN.

| Term | TiN | | Term | VN | |
|-------------|-------|-------|-------------|-------|-------|
| | HF | RESC | | HF | RESC |
| $1^1\Sigma$ | 6.168 | 6.327 | $1^2\Sigma$ | 9.04 | 8.99 |
| $1^3\Sigma$ | 8.508 | 8.641 | $1^2\Pi$ | 9.93 | 9.82 |
| $^3\Pi$ | 8.602 | 8.765 | $2^2\Sigma$ | 10.14 | 10.09 |
| $2^1\Sigma$ | 8.736 | 8.865 | $1^4\Pi$ | 10.35 | 10.11 |
| $1^1\Pi$ | 8.826 | 8.999 | $2^2\Pi$ | 10.84 | 10.59 |

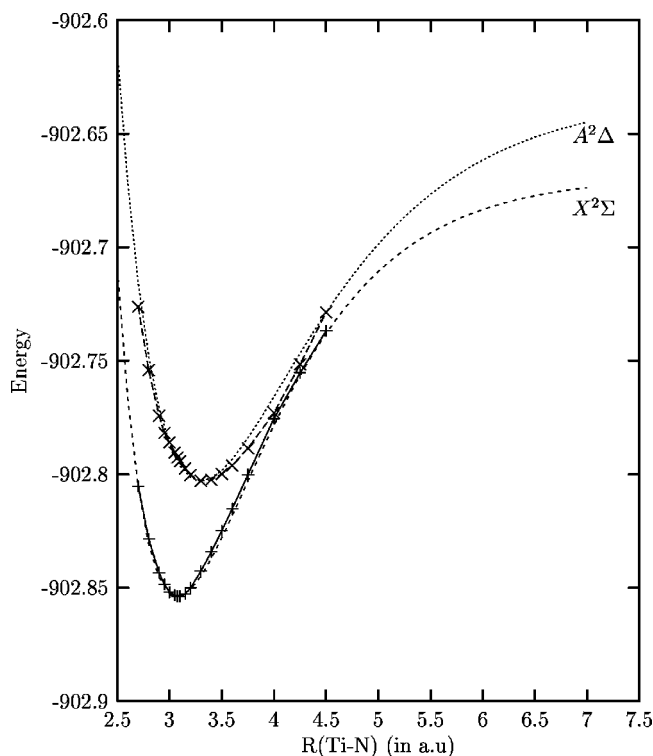


FIG. 1. Plot of ground $X^2\Sigma$ (dashed line) and excited $A^2\Delta$ state (dotted line) potential energy curve of TiN. Lines with cross represent the fitted (Morse) curve.

energy curves of TiN for the ground ($X^2\Sigma$) and first excited states $A^2\Delta$ as a function bond length. The points provide the computations, while the curves are fits of Morse potentials to the data. The computed equilibrium bond length (R_e), vibrational frequency (ω_e), and dissociation energy (D_e) from the two potential energy curves are compared with experiment and with other theoretical data in Table IV. The IVO-CASCI potential energy curves of TiN are computed with Watcher's basis and with 7-valence electron, 7-valence orbital CAS. The ground state of Ti is $^3F\ 3d^24s^2$, and, therefore, it is unlikely that this configuration can lead to triple bond formation. Rather, the next lowest excited state $^5F\ 3d^34s^1$ can couple to produce the TiN ground state. The experimental atomic splitting between the 3F and 5F atomic states of Ti is 0.809 eV (averaged over m_j values). Since this splitting is non-negligible, the computed dissociation energy D_e should be determined by subtracting the 3F - 5F experimental atomic splitting from the asymptotic large R energy. Our theoretically estimated spectroscopic constants are in good agreement, except for the equilibrium bond length. The inaccuracy in the estimated equilibrium bond length, in part, is due to the use of a first order IVO-CASCI approximation and is consistent with the type of behavior expected for CASCI calculations. A similar overestimation of R_e appears in our IVO-CASCI calculations for the ground state of the HF molecule, a deficiency that is rectified by third order H^v calculations.¹⁸ Since our focus here is mostly on vertical excitation energies and ionization potentials, dipole moments, and the comparison between relativistic and nonrelativistic orbitals, we have not carried out third order calculations for the full potential curves of TiN.

To verify that our ground state potential curve for TiN properly fragments into the appropriate Ti and N atomic states, we compute the IP and transition energy of TiN at large internuclear separations R . If TiN dissociates properly, then the above procedures should give the IP and excitation energies of the Ti atom. (The IP of the N atom is much higher than that of the Ti atom.) The computed IP and the 5F - 3F atomic splitting for Ti in TiN at $R=3R_e$ are 6.31 eV and 0.877 eV, respectively. The present overestimation for the 5F - 3F atomic splitting of Ti by 0.072 eV is quite reasonable and suffices to establish the dissociation limit.

B. VN

The ground and excited state properties of VN are computed at the experimental ground state geometry ($R_e = 1.566\ \text{\AA}$) with a "valence triple zeta" basis (66 CGTO). Because of quasidegeneracy between the high (low) lying occupied (unoccupied) orbitals, we include four occupied ($1\delta, 3\pi, 8\sigma$) and three unoccupied orbitals ($9\sigma, 4\pi$) in our reference space. (In accord with Harrison,²⁶ the "1 δ " orbital is actually a nondegenerate orbital with primarily d character.)

Table V compares the vertical transitions energies obtained from H_v^{3rd} theory with the experiment and with other theoretical calculations. In contrast to previous theoretical investigation, the present calculations indicate the possible existence of few low lying excited state of Σ and Π symmetry that have not been considered previously. One computation of the H^v trivially enables computations for low lying states of all symmetries, whereas many widely used schemes, such singles and doubles configuration interaction (SDCI), limited multiconfiguration SCF (MCSCF) methods, etc., require separate full scale calculations for each symmetry. It is also interesting to note that the state energies computed with RESC orbitals are to some extent more accurate than those obtained from the HF orbitals.

C. Positive ion states of TiN and VN

Table VI summarizes the calculated H_v^{3rd} vertical ionization potentials (IPs) of TiN and VN. The IPs reported in Table V are computed with Watcher's basis at the experimental geometry. To our knowledge, neither the experimental nor computed IPs of TiN and VN are available to assess accuracy of the calculated IPs. However, since our computed transition energies and spectroscopic constants are in accord with the experiment and with other theoretical estimates, we strongly believe our calculated IPs represent a very good prediction, especially in view of prior accurate IPs from numerous other H^v calculations.^{22,23}

IV. CONCLUDING REMARKS

Multireference many-body perturbative schemes (IVO-CASCI and H_v^{3rd}), which are applicable to the direct calculation of excitation energies (EE), ionization potentials (IP) and related properties, are applied to compute the transition energies, ionization potentials, and spectroscopic constants of TiN. Highly satisfactory results are obtained for the excitation energies and for the dissociation energy, dipole moments, oscillator strengths, and vibrational frequencies. Ver-

tical excitation energies and IPs are likewise computed for VN. The computations include several states that have not previously been studied. The ground and excited properties are also computed with MOs obtained from two-component Dirac–Hartree–Fock equations to assess the importance of (the expected small) relativistic effects as a prelude to treating systems where the relativistic contributions are anticipated to be more significant. Molecular calculations with the four-component Dirac–Hartree–Fock MOs are in progress.

ACKNOWLEDGMENT

This research is supported, in part, by NSF Grant No. CHE9727655.

- ¹J. C. Philips and L. Kleinman, *Phys. Rev.* **116**, 287 (1959).
- ²S. Huzinaga, L. Seijo, Z. Barandiran, and M. Klobukowski, *J. Chem. Phys.* **86**, 2132 (1987); L. Seijo, Z. Barandiran, and S. Huzinaga, *ibid.* **91**, 7011 (1989).
- ³T. Nakajima, T. Suzumura, and K. Hirao, *Chem. Phys. Lett.* **304**, 271 (1999); T. Suzumura, T. Nakajima, and K. Hirao, *Int. J. Quantum Chem.* **75**, 757 (1999); T. Nakajima, K. Koga, and H. Hirao, *J. Chem. Phys.* **112**, 10142 (2001); K. Motegi, T. Nakajima, K. Hirao, and L. Seijo, *ibid.* **114**, 6000 (2001).
- ⁴P. C. R. J. Buenker and B. A. Hess, *Chem. Phys.* **84**, 1 (1984).
- ⁵T. Nakajima and K. Hirao, *Chem. Phys. Lett.* **302**, 383 (1999).
- ⁶K. F. Freed, in *Lecture Notes in Chemistry*, edited by U. Kaldor (Springer-Verlag, Berlin, 1989), Vol. 52, p. 1.
- ⁷B. H. Brandow, *Rev. Mod. Phys.* **39**, 771 (1967).
- ⁸I. Lindgren, *J. Phys. B* **7**, 2441 (1974).
- ⁹X.-C. Wang and K. F. Freed, *J. Chem. Phys.* **86**, 2899 (1987).
- ¹⁰R. L. Graham and K. F. Freed, *J. Chem. Phys.* **96**, 1304 (1992).
- ¹¹J. P. Finley and K. F. Freed, *J. Chem. Phys.* **102**, 1306 (1995).
- ¹²R. K. Chaudhuri, J. P. Finley, and K. F. Freed, *J. Chem. Phys.* **106**, 4067 (1997).
- ¹³J. P. Finley, R. K. Chaudhuri, and K. F. Freed, *J. Chem. Phys.* **103**, 4990 (1995).
- ¹⁴J. P. Finley, R. K. Chaudhuri, and K. F. Freed, *Phys. Rev. A* **54**, 343 (1996).
- ¹⁵S. Wilson, K. Jankowski, and J. Paldus, *Int. J. Quantum Chem.* **23**, 1781 (1983).
- ¹⁶S. Wilson, K. Jankowski, and J. Paldus, *Int. J. Quantum Chem.* **28**, 525 (1986).
- ¹⁷D. M. Potts, C. M. Taylor, R. K. Chaudhuri, and K. F. Freed, *J. Chem. Phys.* **114**, 2592 (2001).
- ¹⁸R. K. Chaudhuri, K. F. Freed, S. A. Abrash, and D. M. Potts, *J. Mol. Struct.: THEOCHEM* **83**, 547 (2001).
- ¹⁹A. J. H. Wachters, *J. Chem. Phys.* **52**, 1033 (1970); IBM Technical Report RJ584, 1969; C. W. Bauschlicher, Jr., S. R. Langhoff, and L. A. Barnes, *J. Chem. Phys.* **91**, 2399 (1989).
- ²⁰T. H. Dunning, Jr., *J. Chem. Phys.* **90**, 1007 (1989).
- ²¹R. K. Chaudhuri, A. Mudholkar, K. F. Freed, C. H. Martin, and H. Sun, *J. Chem. Phys.* **106**, 9252 (1997).
- ²²R. K. Chaudhuri, K. F. Freed, and D. M. Potts, in *Low-Lying Potential Energy Surfaces*, 828, edited by M. R. Hoffman and K. N. Dylla (Oxford Press, North Carolina, 2002), p. 154.
- ²³J. E. Stevens, R. K. Chaudhuri, and K. F. Freed, *J. Chem. Phys.* **105**, 8754 (1996).
- ²⁴T. M. Dunn, K. L. Hanson, and R. A. Rubinson, *Can. J. Phys.* **48**, 1657 (1970).
- ²⁵B. Simard, H. Niki, and P. A. Hackett, *J. Chem. Phys.* **92**, 7012 (1990).
- ²⁶J. F. Harrison, *J. Phys. Chem.* **100**, 3513 (1996).
- ²⁷C. W. Bauschlicher, *Chem. Phys. Lett.* **100**, 515 (1983).
- ²⁸S. M. Mattar, *J. Phys. Chem.* **97**, 3171 (1993).
- ²⁹K. Brabharan, J. A. Coxon, and A. N. Yamashita, *Spectrochim. Acta, Part A* **41**, 847 (1985).
- ³⁰J. K. Bates, N. L. Ramieri, and T. M. Dunn, *Can. J. Phys.* **54**, 915 (1976).
- ³¹R. A. Gingirich, *J. Chem. Phys.* **49**, 19 (1968).
- ³²A. W. Douglas and P. M. Veilleti, *J. Chem. Phys.* **72**, 5378 (1980).